International Journal of Applied Pharmaceutics

ISSN- 0975-7058 Vol 14, Issue 5, 2022

Original Article

PREPARATION AND EVALUATION OF IGURATIMOD ORAL FORMULATION USING CYCLODEXTRIN NANOSPONGES

MADHAVI M.[1*], SHIVA KUMAR G.[2]

[1,2]GITAM School of Pharmacy, GITAM Deemed to be University, Hyderabad 502329, Telangana, India
*Email: 121965201020@gitam.in

Received: 31 Jan 2022, Revised and Accepted: 15 Jun 2022

ABSTRACT

Objective: Cyclodextrin nanosponges have unfolded themselves as budding delivery aids for intractable molecules that face difficulty in formulation.

Methods: The present research aimed at the preparation of cyclodextrin-based nanosponges employing diphenyl carbonate crosslinker as reported elsewhere. Box-Behnken design was adopted to evaluate the effects of factors (reaction temperature, reaction time and stirring speed) on practical yield and particle size. Based on a numerical optimization technique, five batches of nanosponge formulations with varying molar ratios (1:2, 1:4, 1:6, 1:8 and 1:10) were formulated and evaluated.

Results: The drug loading into optimized β–CD (NS14, NS16) was carried out by by freeze-drying method with a maximum drug loading of 32% displayed by IGNS14. The particle sizes of Iguratimod-loaded nanosponges range between 178 to 181 nm with lower polydispersity indices. The formulation IGNS14 and IGNS16 displayed optimal zetapotential of-27 and-26 mV, which is sufficient to stabilize the colloidal nanosuspension. The dissolution of both nanosponges was significantly higher (>98%) and controlled when compared to pure drug (34%). Retention of the drug in the optimized nanosponges was observed, which was released slowly over time. The PXRD confirm the formation of paracrystalline nanosponges that are spherical in shape with no interaction amongst the drug and excipients.

Conclusion: The cyclodextrin-based NS of Iguratimod were a probable alternative for drug delivery with improved physicochemical properties and therapeutic efficacy.

Keywords: Iguratimod, Rheumatoid arthritis, Cyclodextrin-based nanosponges, Box-Behnken design

DOI: https://dx.doi.org/10.22159/ijap.2022v14i5.45044. Journal homepage: https://innovareacademics.in/journals/index.php/ijap

INTRODUCTION

Nanosponges (NS) are novel hyper-cross-linking structures based on the polymer that consist of solid nanoparticles of colloidal size and nanosized cavity. Cyclodextrin-based nanosponges (β-CD) facilitate prolonged drug release, improved bioavailability by modification of the pharmacokinetic parameters of the drug. Nanosponges have been comprehensively studied as solubilising agents, chemical stabilizers, permeability enhancers, ocular delivery and as a means of increasing cytotoxicity [1]. They are competent in keeping up with advancements in nanomedicine, responding optimistically towards the needs of targeted treatments that aim to enhance the drug efficacy and reduce adverse effects [2].

β-CD have attracted the attention of researchers for resolving major bioavailability issues, including inferior solubility, inferior dissolution rates and limited stability of few agents, along with increasing the drug effectiveness and reducing undesirable side effects [3]. These are hyper-branched polymers researched in the last few years and are easily prepared by reaction between cyclodextrin and a suitable cross-linking agent such as carbonyldimidazole (CDI) [4]. The β–CD displayed an enhanced complexing facility when compared to natural cyclodextrins towards various drugs [5-7].

Iguratimod discovered by Toyama Pharmaceuticals; developed with Eisai (Japan), got approval by Japanese PMDA (Pharmaceuticals and Medical Devices Agency) in 2012 for the management of rheumatoid arthritis. Its mechanism includes inhibitory activity on T and B lymphocytes and other cytokines responsible for inflammation. Additionally, this drug possessed anabolic effect on metabolism of bone, via osteoblastic differentiation stimulation and osteoclast genesis inhibition.

Even though drugs being a novel DMARD have been effective in disease management; its, side effects like an increase in the level of liver enzymes and gastrointestinal irritation were main disturbing features in clinical practice. The drug exhibits practical insolubility in aqueous solvents and is administered orally only. Various factors are influence rate and extent of intestinal drug absorption that result in decreased clinical effectiveness and increased GIT side effects. A novel formulation is the need of the hour to decrease drug side effects and increase its bioavailability that would aim at promising management of RA [8-10].

The current research is aimed to formulate inclusion complexes of Iguratimod in β-CD resulted in improved solubility and dissolution.

MATERIALS AND METHODS

Material

β-Cyclodextrin (β-CD) and Iguratimod were gifted by Gangwal Chemicals Pvt. Ltd. (Mumbai, India) and Dr. Reddy's Lab. Ltd., India. Diphenyl carbonate (DPC), Glutaraldehyde (25% Aqueous Solution) was obtained from Sigma Aldrich (Italy). Dialysis membrane (Molecular weight cut off 12 kDa) was from Hi-media Pvt. Ltd.,

Formulation of β-CD

The β-CD nanosponges were prepared with the aid of crosslinker diphenylcarbonate as reported elsewhere [5]. Following procedure was followed for the process as shown in fig. 1, with reactions conditions as specified in table 1.

Optimization of reaction conditions by experimental design

Exploratory experimentation at initial stages was carried out for determination of main factors and their appropriate optimal range. The influence of three factors on percentage yield (PY) and particle size (PS) were checked and notified as the most critical ones within range of 90-110 °C, 300-420 min, 2000-5000 rpm, respectively.

A 3-factor, 3-level Box-Behnken design (BBD) was utilized for studying independent variable impact on dependent variables (PY; PS) [11, 12]

Table 1 lists out the level ranges of each independent and dependent variables employed in the model. Table 2 represents the dependent variables responses. Stat-Ease Design Expert® software V8.0.1 was employed for data analysis.

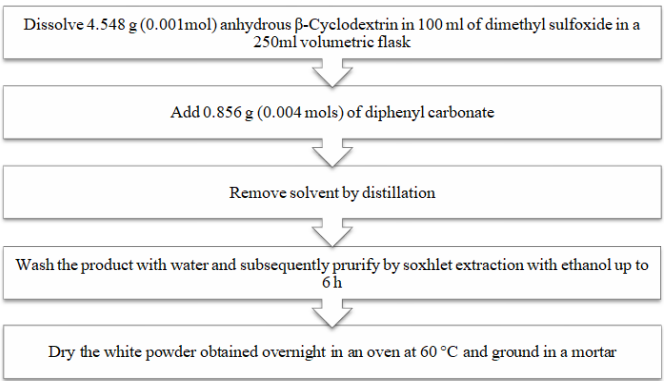

Fig. 1: Flow chart for preparation of β-CD

Table 1: **List of dependent and independent variables in BBD**

Independent variables			Levels		
Variable		**Units**	**Low**	**Intermediate**	**High**
A	Reaction temperature	°C	90	100	110
B	Reaction time	Min	300	360	420
C	Stirring speed	RPM	2000	3500	5000
Dependent variables			Goal		
Y1	Practical yield	%	Maximize		
Y2	Particle size	Nm	Minimize		

Table 2: The BBD experimental design and responses

Run	RT (°C)	RCT (min)	SS (rpm)	PY (%)	PS (nm)
1	110	360	5000	91.23	153.12
2	100	360	3500	93.45	151.34
3	90	300	3500	82.35	223.42
4	100	300	5000	93.88	198.72
5	90	360	2000	77.36	245.67
6	90	360	5000	83.42	226.23
7	100	300	2000	88.34	224.45
8	100	360	3500	92.88	151.79
9	110	300	3500	90.43	190.82
10	90	420	3500	80.84	208.56
11	110	420	3500	89.73	176.12
12	100	360	3500	93.76	150.73
13	100	420	5000	94.56	151.23
14	100	420	2000	89.72	243.76
15	110	360	2000	86.53	252.67
16	100	360	3500	92.93	150.72
17	100	360	3500	93.75	152.26

Table 3: Molar concentration of CD and DPC

S. No.	Code	Molar ratio	Amount of CD (g)	Amount of DPC (g)
1	NS12	1:2 (β-CD: DPC)	4.548	1.712
2	NS14	1:4 (β-CD: DPC)	4.548	3.424
3	NS16	1:6 (β-CD: DPC)	4.548	5.136
4	NS18	1:8 (β-CD: DPC)	4.548	6.848
5	NS110	1:10 (β-CD: DPC)	4.548	8.56

Evaluation of nanosponges

The PY

Following equation was employed for the calculation of each batch's PY relative to the theoretical yield

$$\text{Percentageyield} = \frac{\text{Mass of actual yield}}{\text{Mass of theoretical yield}} \times 100\%$$

The PS

Mastersizer 2000 (Malvern Inst. Ltd, UK) was used for the measurement of PS range and PDI uniformity of NS. Presented data is the means of averages of three independent samples manufactured under similar conditions of production. Milli Q water was used for appropriate sample dilution before measurement.

Data analysis

Linear, cubic and quadratic models describe the relationship allying dependent and independent variables for a BBD. A p value<0.001 was set up for significant terms. Selection of an acceptable fitting model was done by comparison of various statistical parameters, like p-value (p<0.001), p value of lack of fit (p>0.001), the multiple correlation coefficient (R2), adjusted R2, and the coefficient of variation proved by Stat-Ease Design Expert® software V8.0.1. Quadratic models were used

to evaluate individual response parameters for each response parameter using the multiple linear regression analysis.

Optimization and confirmation experiments

Development of a stable process was done by establishing restraints on all the variables. In addition, 5 extra confirmation experiments with both ingredients varying molar concentrations were performed for verification of statistical experimental strategies validity. Reactants molar ratios of five varied types of NS are shown in table 3.

Characterization of nanosponges

Fourier transformed infrared (FTIR) spectroscopy

The FTIR recording was performed by KBr disc technique on a Tensor 27 Spectrophotometer (Bruker Optics, Germany) between 4000 to 600 cm−1.

Differential Scanning Calorimetry (DSC)

DSC study were performed in a Perkin Elmer DSC/7 (CT-USA) fitted with a TAC 7/DX controller.

X-Ray Powder Diffraction (XRPD)

The XRD patterns were recorded on X-ray diffractometer (Bruker D8 Advance) at a scan rate of 5°/min in the 2θ range from 2.5° to 60°.

Iguratimod-loaded β-Cyclodextrin Nanosponge (IGNS) formulation

Freeze drying technique was used to manufacture Iguratimod (IGD) loaded NS [13, 14] About 100 mg of β-CD was suspended in 100 ml of Milli Q water using a mechanical stirrer (REMI). This was followed by addition of 100 mg of drug to the above mixture and further sonication for 10 min to prevent aggregation. The mixture was stirred for 24h. About 20 min centrifugation of the suspension was carried out at 5000 rpm to separate drug that did not undergo complexation. Separation of the colloidal supernatant was done and freeze-dried at-20 °C and 13.33 mbar. Dry powder after lyophilization and stored in desiccators. NS loaded with the drug were labelled as IGNS14 and IGNS16 depending on the type of NS used for loading.

Evaluation of Iguratimod loading in NS

Weighed quantity of drug-loaded NS were subjected to dissolution in carbinol and sonicated for 10 min for breaking complex. Appropriate dilution with methanol was done and then subjects to UV-Visible spectrophotometer analysis at 257 nm. Calculation of IGD content from standard curves was done using formula 1.

$$\% \text{ Drugloading} = \frac{\text{Weight of drug loadedin NS formulation}}{\text{Initial weight of the drug fed for loading}} \times 100 \quad \ldots\ldots\ldots (1)$$

Physico-chemical characterization of plain nanosponges and IGNS

The PS distribution of plain NS and IGD-loaded NS was observed by dynamic light scattering using a 90-plus particle sizer (Brookhaven Instruments Corporation, USA) equipped with MAS OPTION particle sizing software at fixed angle of 90 ° for all samples. Sample dilution Milli Q water was done prior to measurement. An additional electrode in was also used for zeta potential measurement in the same instrument. Experimentation was done in triplicate at 25±2 °C [15, 16].

***In vitro* release of Iguratimod from IGNS**

In vitro dissolution study of IGNS formulations and free IGD was performed using rotating cells containing multiple compartments (n=6) with a dialysis membrane (Sartorius cut off 12,000 Da). The membrane was activated as per the procedure provided by the manufacturer. About 10 mg of IGD equivalent formulation was filled in the dialysis bag and placed in donor phase containing 100 ml simulated gastric fluid (pH 6.4). Same medium was placed in receptor phase with 0.5% w/v sodium lauryl sulphate (1 ml) sink conditions maintenance. Complete withdrawal of receptor phase at 0, 0.25, 0.5, 0.75, 1, 1.5, 2, 3, 4, 6, 8, 12, and 24 h was performed afterwards. Analysis of the samples by UV-visible spectrophotometer at 257 nm was performed after appropriate dilution. The experiment was performed in triplicate.

Kinetic study

Drug release data from *in vitro* was applied to a variety of mathematical release kinetics model for elucidation of mode and drug release mechanism by interpretation in graphical presentation form and evaluated by correlation coefficient (R^2).

Characterization of plain nanosponges and Iguratimod-loaded nanosponges

The surface morphological features of plain NS and IGNS were seen under transmission electron microscopy (JEM-2000 EXII; JEOL, Tokyo, Japan). The FTIR, DSC and PXRD evaluation of Cyclodextrin NS, IGD and IGD-loaded NS was carried as per the procedure adopted for β-CD [16].

RESULTS AND DISCUSSION

Three types of NS (NS1-NS3) were formulated using various ratios of Cyclodextrin and CDI (fig. 2). Following equation described the practical yield as a simultaneous function of RT (A), RCT (B) and SS (C):

$$\text{Practical yield}(Y1) = 93.24 + 4.24A + 2.64B - 7.27A^2 - 1.48C^2$$

The PY ranged from 77.36 to 94.56 %. The generated quadratic model revealed PY to be significantly impacted by levels of RT (A) and SS (C) without producing any interaction. A good similarity was noted between theoretical and observed values. The influence of main and interactive effects of independent variables on the PY was shown using perturbation (PP), contour (CP) and 3D response surface plots (RSP). (fig. 3A, 3B, 3C)

The fig. clearly show that A and C have a major and moderate effect on Y1, respectively.

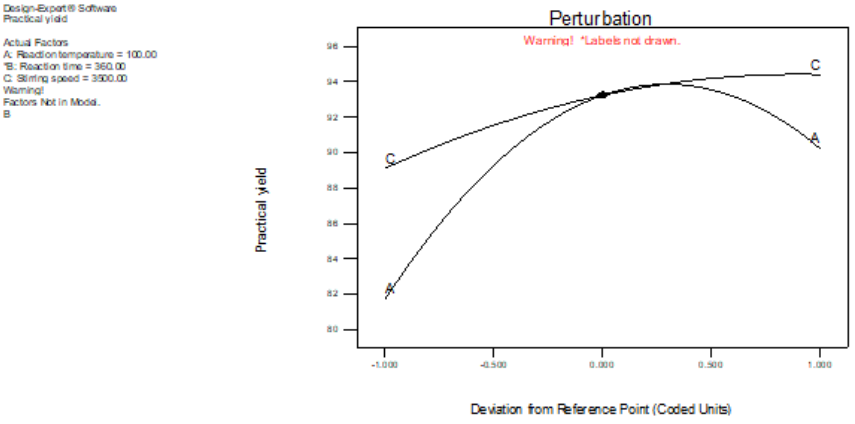

Fig. 3A: The PP showing the main effects of A and C on Y1

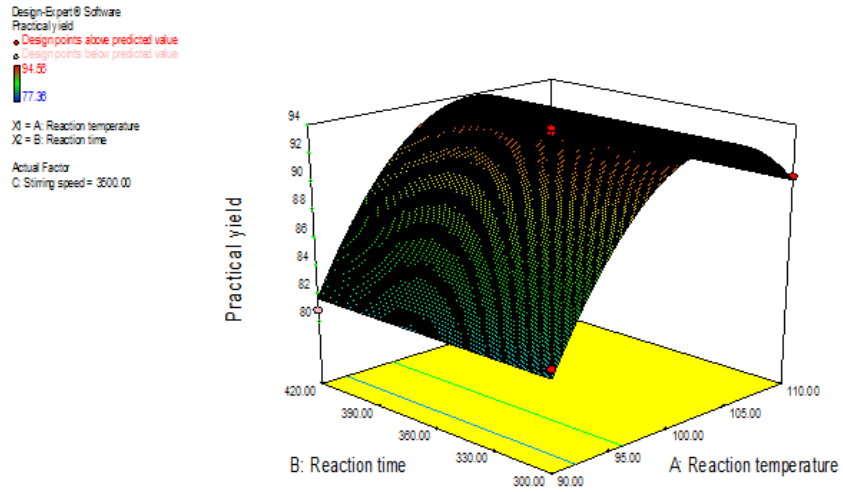

Fig. 3B: RSP displaying the interactive effect of A and B on Y1

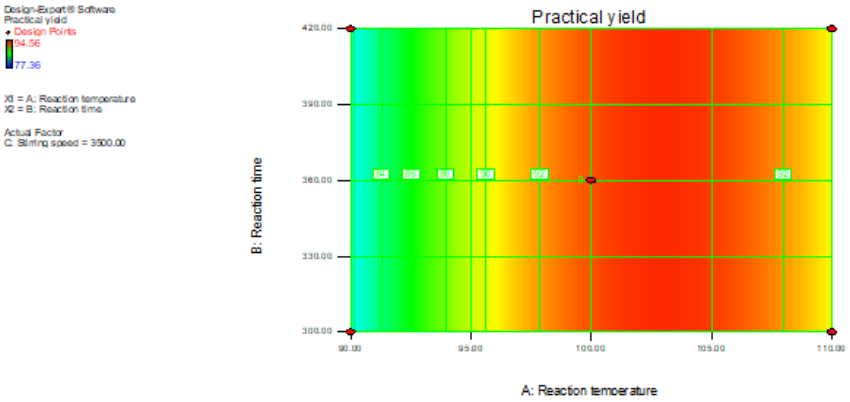

Fig. 3C: CP showcasing the interactive effect of A and B on Y1

Following polynomial equation, describes the mean particle size as a simultaneous function of RT (A), RCT (B) and SS (C), is as shown

$$Meanparticlesize(Y2) = 151.37 - 16.39\,A - 7.22\,B - 29.66\,C - 20.03\,AC - 16.70\,BC + 31.62\,A^2 + 16.74\,B^2 + 36.43C^2$$

PS analysis of NS ranged from 150.72–252.67 nm (table 2). Significant antagonist action of RT (A), RCT (B) and SS (C) on the mean PS was revealed by generated quadratic model. A fair similarity was observed between theoretical (predicted) and observed values.

Independent variables influence on PS was further shown using the three plots (fig. 4A, 4B, 4C, 4D and 4E).

"The fig. show that the main effect of A, B and C on Y2. This fig. is a clear indication that C exhibits major effect on Y2 followed by A and B having a moderate effect on Y2.

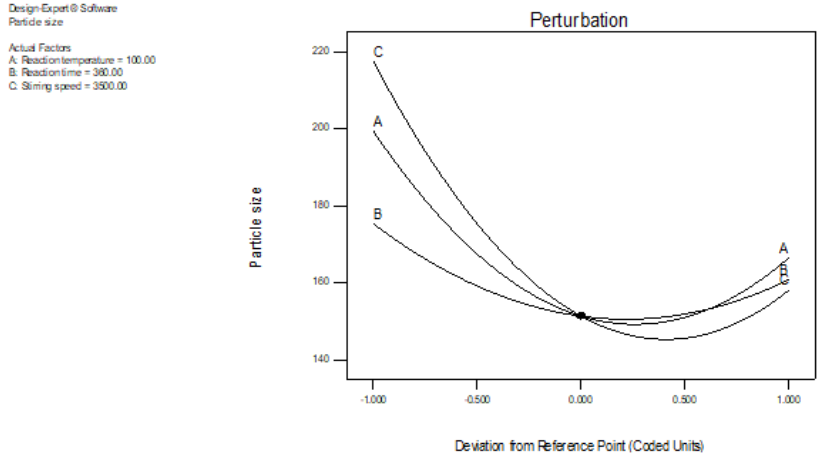

Fig. 4A: PP showcasing the main effects of A, Band con the particle size (Y2)

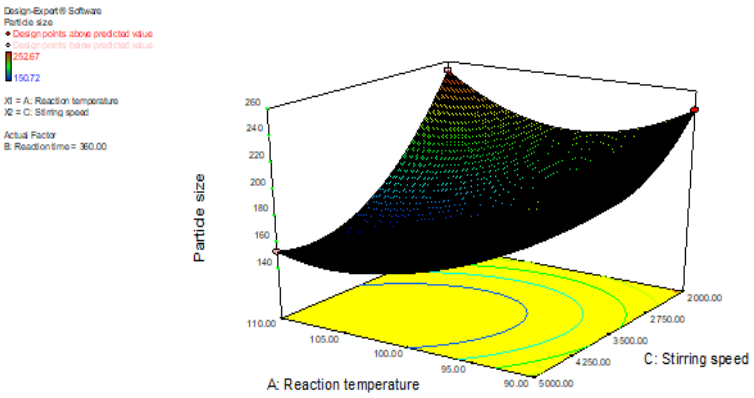

Fig. 4B: RSP showcasing the interactive effects of A and C on PS at a fixed B

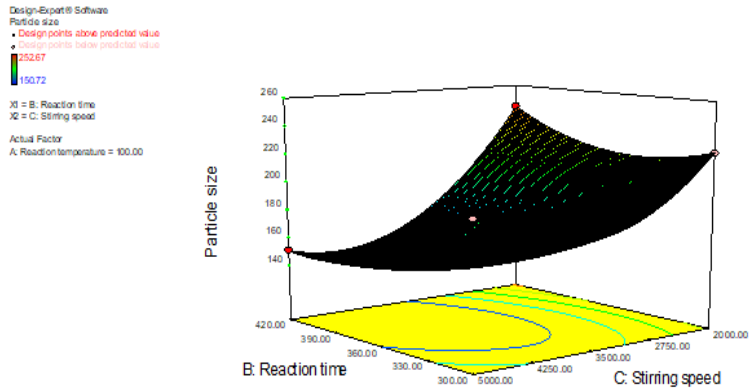

Fig. 4C: RSP showcasing the interactive effect of B and C on PS at a fixed A

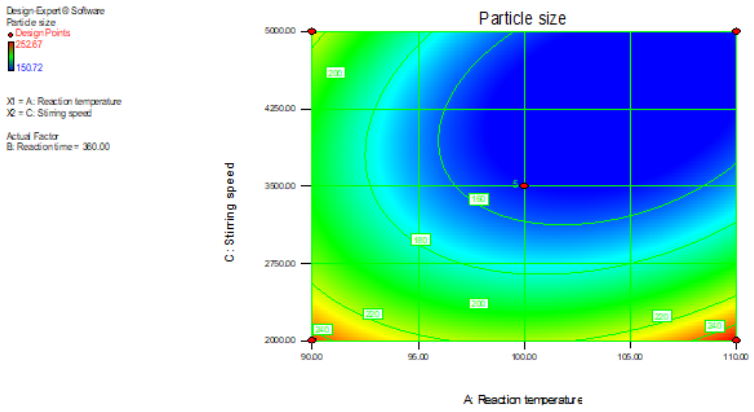

Fig. 4D: CP showcasing the interactive effect of A and C on PS at fixed B

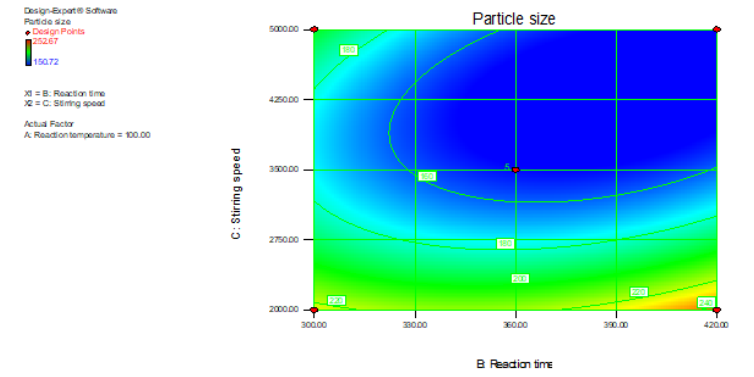

Fig. 4E: CP showing the interactive effect of B and C on particle size at a fixed level of A

Optimization and confirmation experiments

NS with required responses were prepared employing a numerical optimization technique using the desirability approach. The prime settings of independent variables were located by setting constraints like maximizing the PY in addition to minimizing the PS as goals. Table 4 depicts predicted and observed values. A close proximity was observed between obtained Y1 and Y2 values and predicted values. Thus, a clear demonstration of optimization procedure reliability in prediction of the operating parameters NS synthesis was made.

Table 4: Optimized values obtained by the constraints applies on Y1 and Y2

Independent variable	Nominal values	Predicted values		Observed values			
		(Y1)	(Y2)	Batch	PY (Y1)	PS (Y2)	Zeta potential (mV)
RT	103.26	94.79	143.67	NS12	93.12±4.3	151.23±5.2	-25.68±2.1
				NS14	95.34±8.27	143.42±3.8	-26.73±1.2
RCT	349.32			NS16	92.42±9.56	159.76±4.4	-32.46±2.7
				NS18	91.94±3.6	150.72±3.7	-27.34±1.9
SS	4238.73			NS110	94.62±2.2	147.87±5.6	-25.12±2.1

Data is given as mean±Standard Deviation; (n=3)

Characterization of cyclodextrin nanosponges

FTIR studies

FTIR spectra of β-CD depicted a peak at 1740–1750 cm-1, for C=O bond between two β-CD, which is absent in the spectrum of β-CD (fig. 5), which is a starting material for synthesis of NS. Other distinguishing peaks of NS were observed at 2918 cm-1 owing to C-H stretching vibration, 1418 cm-1 owing to C–H bending vibration and 1026 cm-1 owing to C-O stretching vibration of primary alcohol. An increase in main peak intensity at around 1740–1750 cm-1 was observed in NS spectrum due to an increase in cross-linking degree.

XRD studies

Solid structure of NS was characterized by X-ray analysis. A crystalline structure was noted in plain β-CD (not cross-linked) in fig. 6. A weak long-range ordered crystalline degree was observed in XRPD pattern of NS characterized by few broader reflections appearing as narrow peaks in the XRPD of β-CD. Formation of paracrystalline NS is indicated by the absence of short-range order and the presence of some broad reflections. Similar XPRD patterns were noted among different batches of NS synthesized using various cross-linking ratio.

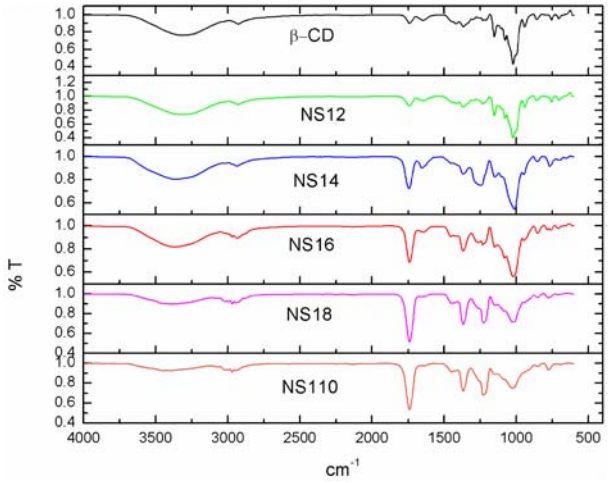

Fig. 5: FTIR spectra of β-CD and NS

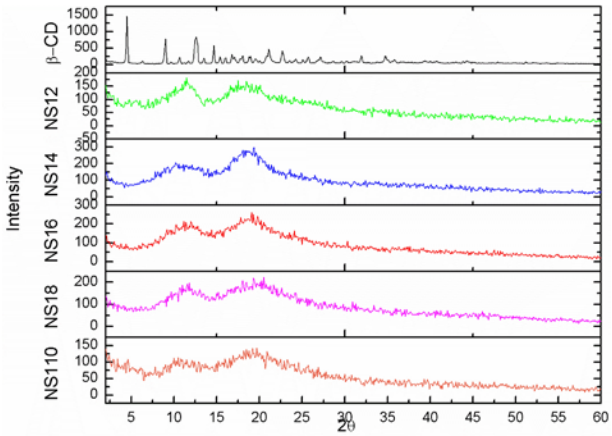

Fig. 6: XRD pattern of *β*-CD and NS

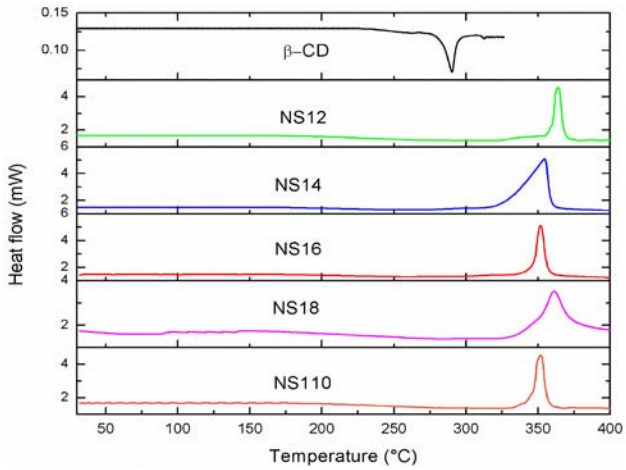

Fig. 7: DSC thermograms of *β*-cyclodextrin and cyclodextrin nanosponges

DSC studies

The DSC thermogram of β-CD displayed an endothermic peak at 290 °C that corresponded to the melting transition point (fig. 7). Absence of peaks before 350 °C from DSC of NS indicated high thermal stability of the material.

Iguratimod loading in cyclodextrin nanosponges

IGD was loaded into the NS by freeze drying method. IGD was loaded into two types of NS (NS14 and NS16) considering their solubilization potential. After lyophilization the dry powder obtained was stored in a desiccator. The drug-loaded NS were designated as IGNS14 and IGNS16 depending on the NS type used for loading. Drug association with NS was determined drug loading measurement from a fixed formulation amount and the percent drug loaded was calculated as specified previously. Percent drug loading into both types of NS (IGNS14 and IGNS16) were presented in table 4.

It was found that for the β-CD nanosponge, A high drug loading was observed in NS14 (1:4 β-CD: DPC) as much as 32.5 % w/w, while 28 %was loaded in NS16 (1:6 β-CD: DPC). A high concentration of cross linker might have resulted in hyper cross liked β-CD, resulting in a hindered interaction of drug with β-CD cavities. This clearly proves that the amount of cross linker is a critical factor in determining drug loading into NS (table 5).

Table 5: % Drug loading of NS

S. No.	Name of the formulation	Drug loading (%)	Cumulative variance (%)
1	IGNS14	32.5	0.43
2	IGNS16	28	0.89

Physico-chemical characterization of Iguratimod-loaded nanosponges

The particle size analysis of IGNS14 and IGNS16 suspensions indicated average particle size in range of 178–182 nm with low PDI. The particle size distribution was found to be unimodel and having a narrow range as seen in the table 6. A sufficiently high zeta potential indicates that the complexes would be stable and the tendency to agglomerate would be miniscule. A narrow PI means that the colloidal suspensions are homogenous in nature.

Table 6: PS analysis of Iguratimod-loaded nanosponges

Sample	PS±SD (nm)	PDI	Zeta potential (mV)
NS14	143.42±8.27	0.19±0.005	-26.73±1.2
NS16	159.76±9.56	0.24±0.005	-32.46±2.7
IGNS14	181.52±4.54	0.26±0.005	-27.34±1.4
IGNS16	178.12±9.34	0.23±0.005	-26.12±2.1

Data is given as mean±standard deviation; (n=3)

***In vitro* dissolution of Iguratimod from NS formulations**

In vitro dissolution pattern of IGD was evaluated from nanosponge formulations (IGNS14 and IGNS16) and free IGD suspension in the simulated gastric medium is shown fig. 8. More than 95 % of the drug was found to be released from nanosponge formulations as compared to only around 34 % from free drug suspension after 24 h of study. *In vitro* release study of IGD from IGNS16 formulation showed sustained drug release. A slow-paced sustained release of drug indicates diffusion of IGD from within the entrapped NS inclusion complex. The nanosponges (IGNS14) of the lower degree of cross-linking have shown initial rapid burst release and around 38 % of the drug was release within 60 min. This was normally attributed to the fraction of Iguratimod which was adsorbed or encapsulated as a non-inclusion complex on the surface of nanosponges. Upon the addition of the formulation to the release medium, this fraction of the drug was diffused rapidly into the surrounding liquid. Similarly, the nanosponges with a higher degree of cross-linking (IGNS16) have shown a biphasic release pattern of Iguratimod. The observed initial burst release was might be due to the Iguratimod, which is present in the matrix form but not associated with the inclusion complex. Subsequently, sustained release of the drug was observed due to the presence of the drug in the inclusion complex.

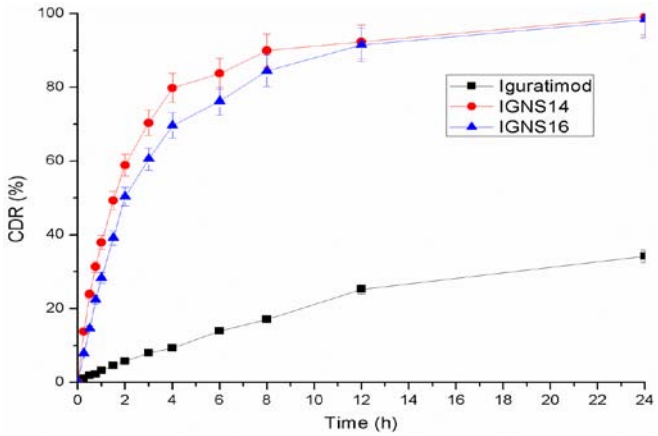

Fig. 8: Dissolution profile of pure Iguratimod and Iguratimod loaded nanosponge formulations, Data is given as mean±standard deviation; (n=3)

Characterization of iguratimod NS

FTIR analysis

Absence and broadening of peaks from FTIR of drug-loaded complex is indicative of weak interaction between drug and NS. Comparison of IGD FTIR spectra with that of NS complex manifested a major change in. 900 to 1,400 cm-1. The main characteristic peaks of IGD are at around 3423, 3347, 3276, 3123, 3065, 2869, 1687, 1620, 1592, 1531, 1487, 1425, 1358, 1342, 1264, 1210, 1155, 970 and 757 cm-1 that were absent from that of complex formulations indicating the inclusion complexation between IGD and NS as mentioned in reported reference [17] (fig. 9).

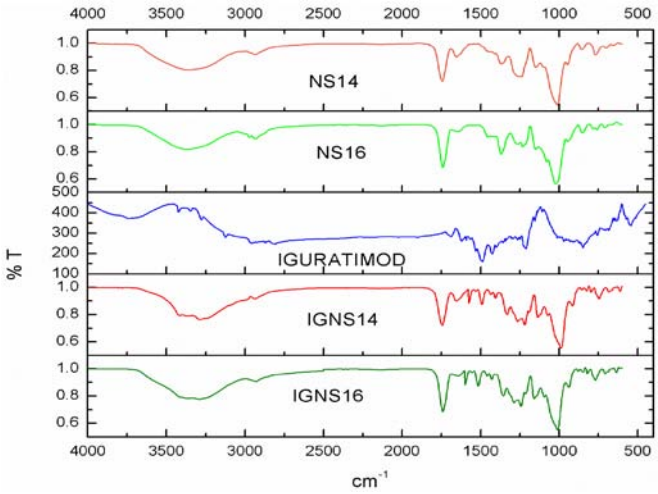

Fig. 9: FTIR spectra of NS14, NS16, Iguratimod, IGNS14 and IGNS16

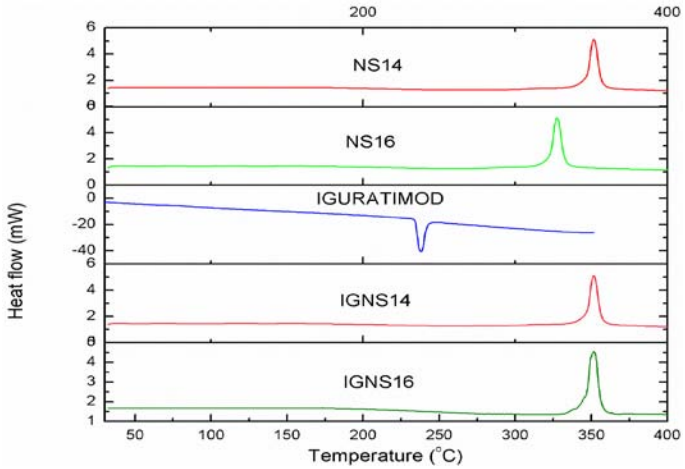

Fig. 10: The thermograms of NS14 and NS16, Iguratimod and Iguratimod loaded nanosponge complexes (IGNS14 and IGNS16)

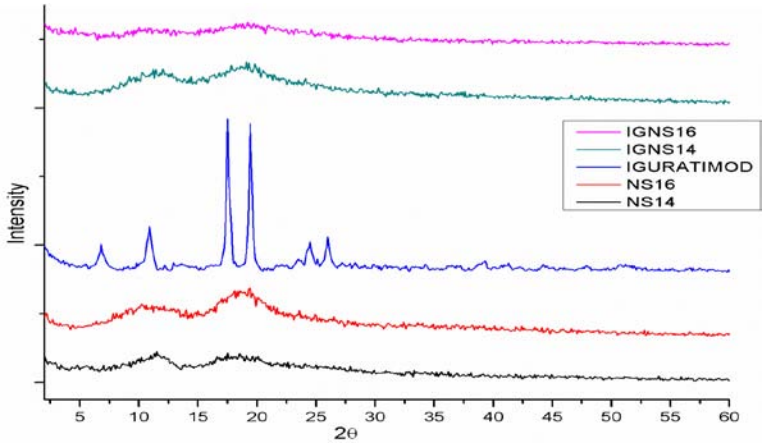

Fig. 11: XRPD pattern of plain nanosponges (NS14 and NS16), Iguratimod and Iguratimod loaded nanosponge complexes (IGNS14 and IGNS16)

DSC

DSC curves of the free IGD, plain NS (NS14 and NS16) and IGD loaded NS complexes (IGNS14 and IGNS16) are displayed in fig. 10. Drug crystalline nature is shown by the presence of sharp endothermic peak at 238.51 °C in DSC thermogram of free drug. The DSC thermogram of plain NS (NS14 and NS16) showed exothermic peaks at around 350 °C. IGD-loaded NS complex (IGNS 14 and IGNS16) also had a broad exothermic peak at around at 350 °C [18].

X-ray powder diffraction (XRPD)

Physical nature of IGD within the CS was observed. XRD of pure IGD, plain NS (NS14 and NS16) and IGD loaded NS complexes (IGNS14 and IGNS16) were checked. The x-ray diffractograms of plain IGD exhibited sharp intense peaks at 2θ values of 6.88°, 10.92°, 17.54°, 19.56°, 20.8°, 24.56° and 26.00 °C. Confirming the drug crystallinity as shown in fig. 11. No characteristics peak of pure IGD was observed in both the NS complexes (IGNS14 and IGNS16). Drug encapsulation in NS is confirmed by the absence of such crystalline peaks of IGD NS complex, as reported previously.

CONCLUSION

Nanosponges are one of the recently advanced drug delivery systems with sponge-like structures that entrap drug molecules to form an inclusion complex. This study involves designing of two types of nanosponges from β-cyclodextrin (NS14 and NS16) were purposely designed. Iguratimod loading into nanosponges was done by the freeze-drying method. The particle sizes of Iguratimod NS ranged within 178 to 181 nm with low PDI values. Zeta potential was optimally higher to get a stable colloidal nanosuspension. Drug interaction with nanosponges was established by FTIR, DSC and XRPD studies. A slow sustained drug release was observed for drug-loaded nanosponges with comparatively higher drug release relative to the pure drug in simulated intestinal fluid (SIF, pH 6.8).

FUNDING

Nil

AUTHORS CONTRIBUTIONS

All authors have contributed equally.

CONFLICT OF INTERESTS

Declared none

REFERENCES

1. Trotta F, Zanetti M, Cavalli R. Cyclodextrin-based nanosponges as drug carriers. Beilstein J Org Chem. 2012;8:2091-9. doi: 10.3762/bjoc.8.235, PMID 23243470.
2. Bhowmik, Himangshu, Venkatesh D, Kuila, Anuttam, Kumar, Kammari. Nanosponges: a review. Int J Appl Pharm. 2018;10:1-10.
3. Venuti V, Rossi B, Mele A, Melone L, Punta C, Majolino D. Tuning structural parameters for the optimization of drug delivery performance of cyclodextrin-based nanosponges. Opi: Expert Verlag. Drug Deliv. 2017;14(3):331-40.
4. Simranjot Kaur, Sandeep Kumar. The nanosponges: an innovative drug delivery system. Asian J Pharm Clin Res. 2019:60-7. doi: 10.22159/ajpcr.2019.v12i7.33879.
5. Trotta F, Cavalli R. Characterization and applications of new hyper-cross-linked cyclodextrins. Compos Interfaces. 2009;16(1):39-48. doi: 10.1163/156855408X379388.
6. Swaminathan S, Vavia PR, Trotta F, Cavalli R, Tumbiolo S, Bertinetti L. Structural evidence of differential forms of nanosponges of beta-cyclodextrin and its effect on solubilization of a model drug. J Incl Phenom Macrocycl Chem. 2013;76(1-2):201-11. doi: 10.1007/s10847-012-0192-y.
7. Chilajwar SV, Pednekar PP, Jadhav KR, Gupta GJC, Kadam VJ. Cyclodextrin-based nanosponges: a propitious platform for enhancing drug delivery. Expert Opin Drug Deliv. 2014;11(1):111-20. doi: 10.1517/17425247.2014.865013, PMID 24298891.
8. Anita Chando, Munira Momin, Mural Q, Shaily L. Topical nanocarriers for management of rheumatoid arthritis: a review. Biomed Pharmacother. 2021;141:111880. doi: 10.1016/j.biopha.2021.111880.
9. Takeba Y, Suzuki N, Wakisaka S, Nagafuchi H, Mihara S, Kaneko A. Effects of actarit on synovial cell functions in patients with rheumatoid arthritis. J Rheumatol. 1999;26(1):25-33. PMID 9918236.
10. Janakiraman K, Krishnaswami V, Rajendran V, Natesan S, Kandasamy R. Novel Nano therapeutic materials for the effective treatment of rheumatoid arthritis-recent insights. Mater Today Commun. 2018 Dec;17:200-13. doi: 10.1016/j.mtcomm.2018.09.011, PMID 32289062.
11. Rangaraj N, Pailla SR, Chowta P, S Nagarjun Rangaraj, Sravanthi Reddy Pailla, Paramesh Chowta. Fabrication of ibrutinib nanosuspension by quality by design approach: intended for enhanced oral bioavailability and diminished fast-fed variability. AAPS PharmSciTech. 2019;20(8):326. doi: 10.1208/s12249-019-1524-7, PMID 31659558.
12. Bowden GD, Pichler BJ, Maurer A. A design of experiments (DoE) approach accelerates the optimization of copper-mediated 18F-fluorination reactions of Arylstannanes. Sci Rep. 2019;9(1):11370. doi: 10.1038/s41598-019-47846-6, PMID 31388076.
13. Anandam S, Selvamuthukumar S. Fabrication of cyclodextrin nanosponges for quercetin delivery: physicochemical characterization, photostability, and antioxidant effects. J Mater Sci. 2014;49(23):8140-53. doi: 10.1007/s10853-014-8523-6.
14. Singireddy A, Subramanian SK. Cyclodextrin nanosponges to enhance the dissolution profile of quercetin by inclusion complex formation. Part Sci Technol. 2016;34(3):341-6. doi: 10.1080/02726351.2015.1081658.
15. Darandale SS, Vavia PR. Cyclodextrin-based nanosponges of curcumin: formulation and physicochemical characterization. J

Incl Phenom Macrocycl Chem. 2013;75(3-4):315-22. doi: 10.1007/s10847-012-0186-9.

16. Zoppi A, Quevedo MA, Longhi MR. Specific binding capacity of beta-cyclodextrin with cis and trans enalapril: physicochemical characterization and structural studies by molecular modeling. Bioorg Med Chem. 2008;16(18):8403-12. doi: 10.1016/j.bmc.2008.08.032, PMID 18771929.
17. Madhuri, Shete, Rajkumar. Formulation and evaluation of gliclazide nanosponges. Solunke, Rahul and Borge, Uday and Murthy, Krishna and Deshmukh. Int J Appl Pharm. 2019;11:181-9.
18. El-Assal MI. Nano-sponge novel drug delivery system as carrier of an anti-hypertensive drug. Int J Pharm Pharm Sci. 2019:47-63. doi: 10.22159/ijpps.2019v11i10.34812.